

## Articulating and Stationary PARSIVEL Disdrometer Measurements in Conditions with Strong Winds and Heavy Rainfall

KATJA FRIEDRICH AND STEPHANIE HIGGINS

*University of Colorado Boulder, Boulder, Colorado*

FORREST J. MASTERS AND CARLOS R. LOPEZ

*University of Florida, Gainesville, Florida*

(Manuscript received 6 December 2012, in final form 24 March 2013)

### ABSTRACT

The influence of strong winds on the quality of optical Particle Size Velocity (PARSIVEL) disdrometer measurements is examined with data from Hurricane Ike in 2008 and from convective thunderstorms observed during the second Verification of the Origins of Rotation in Tornadoes Experiment (VORTEX2) in 2010. This study investigates an artifact in particle size distribution (PSD) measurements that has been observed independently by six stationary PARSIVEL disdrometers. The artifact is characterized by a large number concentration of raindrops with large diameters ( $>5$  mm) and unrealistic fall velocities ( $<1$  m s<sup>-1</sup>). It is correlated with high wind speeds and is consistently observed by stationary disdrometers but is not observed by articulating disdrometers (instruments whose sampling area is rotated into the wind). The effects of strong winds are further examined with a tilting experiment, in which drops are dripped through the PARSIVEL sampling area while the instrument is tilted at various angles, suggesting that the artifact is caused by particles moving at an angle through the sampling area. Most of the time, this effect occurs when wind speed exceeds 20 m s<sup>-1</sup>, although it was also observed when wind speed was as low as 10 m s<sup>-1</sup>. An alternative quality control is tested in which raindrops are removed when their diameters exceed 8 mm and they divert from the fall velocity–diameter relationship. While the quality control does provide more realistic reflectivity values for the stationary disdrometers in strong winds, the number concentration is reduced compared to the observations with an articulating disdrometer.

### 1. Introduction

Ground-based disdrometers have been widely used for quantitative precipitation estimation (QPE), in particular to validate radar-derived rainfall rates. Most weather services have upgraded their radar networks to have dual-polarization capability, which requires a constant quality control in order to use dual-polarization measurements for QPE. Ground-based disdrometers can help to maintain a high quality of dual-polarization radar parameters (e.g., Goddard et al. 1982; Goddard and Cherry 1984; Schuur et al. 2001; Berne and Uijlenhoet 2005). Ground-based and airborne disdrometers have also improved our understanding of microphysical processes in precipitation systems such as winter

storms, severe thunderstorms, tropical storms, and hurricanes (e.g., Tokay et al. 1999, 2008; Schuur et al. 2001; Yuter et al. 2006; Thurai et al. 2010, 2011). Recently, mobile disdrometers have been used for the collection of in situ microphysical data in thunderstorms during the second Verification of the Origins of Tornadoes Experiment (VORTEX2) in 2009 and 2010 (Wurman et al. 2012; Friedrich et al. 2013). Disdrometer observations have also been utilized to assess the impact of raindrop size distributions on soil erosion (e.g., Hall and Calder 1993; Coutinho and Tomás 1995; and references within) and in the study of the spatial deposition of wind-driven rain on buildings (Lopez et al. 2011). In particular, during extreme wind events such as landfall hurricanes and cyclones, the location of maximum wetting on the building façade (related to raindrop size and wind speed) directly influences the water penetration into the building. Thus, studies of the raindrop size distribution have an important impact on the development of

---

*Corresponding author address:* Dr. Katja Friedrich, ATOC, University of Colorado Boulder, UCB 311, Boulder, CO 80309.  
E-mail: katja.friedrich@colorado.edu

water penetration resistance requirements of building products. Given the myriad of scientific uses of disdrometer measurements, it is essential that the disdrometers' limitations are categorized and evaluated.

Impact (e.g., Joss–Waldvogel disdrometer) and two-dimensional video disdrometers (2DVD) have historically served as benchmark instruments for measuring raindrop and particle size distributions (DSDs and PSDs). More recently, small lightweight and inexpensive optical disdrometer systems [e.g., previously PM-Tech's and now OTT's Particle Size and Velocity (PARSIVEL) disdrometer] have become a viable option for weather services and research institutions (e.g., Krajewski et al. 2006; Yuter et al. 2006; Brawn and Upton 2008; Lyth 2008; Crewell et al. 2008; Matrosov et al. 2009; Moisseev et al. 2009; Battaglia et al. 2010; Jaffrain and Berne 2011; Niu et al. 2010; Thurai et al. 2010, 2011; and references within). The instruments enable a portable low-cost solution to collecting PSD measurements while yielding qualitatively similar data to video and impact disdrometer measurements in limited data comparison experiments (e.g., Tokay et al. 2001; Caracciolo et al. 2006; Krajewski et al. 2006; Battaglia et al. 2010; Thurai et al. 2011).

Recent studies have begun to examine the performance of PARSIVEL disdrometers in various weather conditions. Jaffrain and Berne (2011) investigated the sampling uncertainty of the OTT PARSIVEL disdrometers using 15 months of data during light and moderate rainfall in Switzerland. They found that the sampling uncertainty for the total concentration of drops and radar reflectivity was 13% and 15%, respectively, for 1-min sampling intervals. During the Disdrometer Evaluation Experiment (DEVEX), Krajewski et al. (2006) compared measurements of three types of disdrometers: PM-Tech PARSIVEL, 2DVD, and a dual beam spectropuviometer. The measurements from the disdrometers were in general agreement, although the PARSIVEL measured a larger number concentration of smaller drops ( $d \sim 0.2\text{--}0.4\text{ mm}$ ) and higher rainfall rates compared to the 2DVD and the pluviometer. Krajewski et al. (2006) hypothesized that the high concentration of smaller drops at low rainfall rates could be related to the instrument's background noise. They further hypothesized that splashing of raindrops and condensation of water vapor on the structure of the instrument and lenses could cause differences between the PARSIVEL and the other instruments. Large differences between the PARSIVEL and the 2DVD occurred primarily when the rainfall rate exceeded  $20\text{ mm h}^{-1}$ ; however, the effects of wind speed and wind direction on the measurement accuracy were not analyzed. Thurai et al. (2011) compared particle size distributions measured

by OTT PARSIVEL disdrometers and 2D video disdrometers during a large variety of precipitation events (e.g., outer hurricane rainband, stratiform rain, convective cells, and organized convective squall lines) in Huntsville, Alabama. Measurements between the PARSIVEL and the 2DVD show close agreement for low rainfall rates ( $<20\text{ mm h}^{-1}$ ), while for larger rain rates the PARSIVEL overestimates rainfall by 20%–30%. Large differences were observed during mixed-phase events when the hydrometeors were not fully melted. While those experiments provide valuable insights into the performance of the PARSIVEL disdrometer, the studies did not address the influence of wind on the measurements. Nešpor et al. (2000) studied the effect of strong wind on measurement accuracy using a 2DVD. In particular, small drops can be deflected before they enter the sampling area under strong wind conditions. During high turbulence, small drops can intersect the measurement area several times, leading to an overestimation of smaller drops.

In this study, we present PSD observations from several OTT PARSIVEL disdrometers in strong winds and heavy rainfall. Data from Hurricane Ike in 2008 and from convective thunderstorms observed during VORTEX2 in 2010 are analyzed to study the impact of strong winds and rainfall rate on the measurement accuracy. While the instrument itself can withstand strong winds and hail, the measurement accuracy seems to be adversely affected by strong winds and turbulence. Section 2 will provide an overview of the measurement principle, data analysis, quality control, and the effect of strong winds on the measurements. Section 3 shows observations from Hurricane Ike and VORTEX2. A comparison between stationary disdrometer and radar observations as well as stationary versus articulating disdrometer measurements together with possible quality-control methods are discussed in section 4. Conclusions are presented in section 5.

## 2. Instruments

### a. PARSIVEL measurement principle

The OTT PARSIVEL optical disdrometers shown in Fig. 1 use a 650-nm laser device with a power of 3 mW (Löffler-Mang and Joss 2000; Löffler-Mang and Blahak 2001). The laser produces a horizontal sheet of light 30 mm wide and 180 mm long (denoted as laser beam in Fig. 2). The horizontal sampling area is nominally  $54\text{ cm}^2$ . Particles passing through the horizontal sampling area cause a reduction of the light intensity that is a measure of particle size (Fig. 2a). The duration of the signal and the particle size allow for an estimate of the

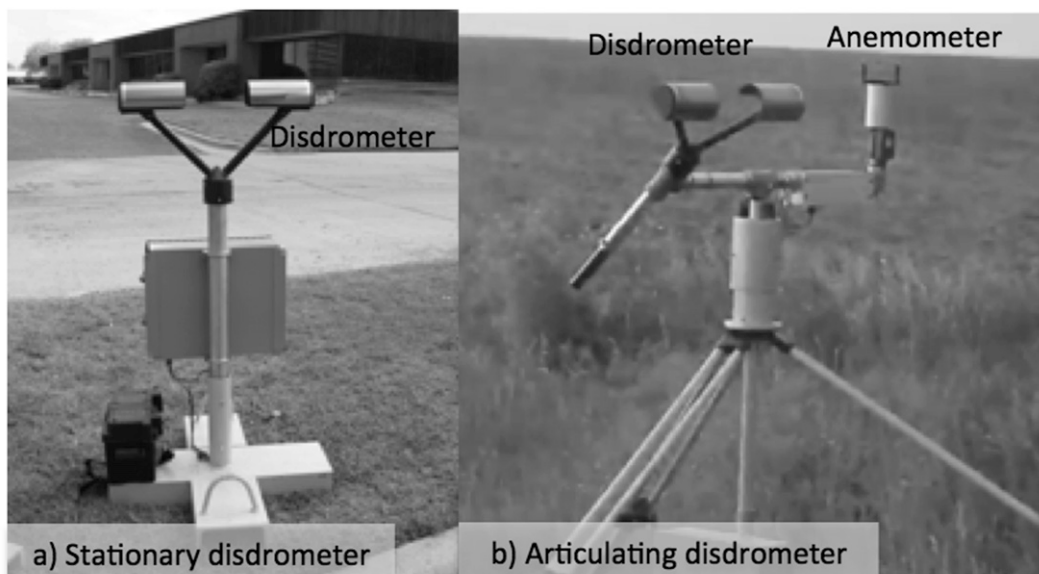


FIG. 1. (a) Stationary and (b) articulating disdrometers deployed during VORTEX2 2010. In (b), motors rotate the articulating disdrometer sampling area into the wind based on measurements from the anemometer.

particle velocity with the assumption that the particles are spheres (Fig. 1 in Löffler-Mang and Joss 2000). The size and fall velocity of each particle are sorted into 32 velocity classes ranging from 0.05 to 20 m s<sup>-1</sup> and 32 particle size classes ranging from 0.062 to 24.5 mm. Note that the instruments used in the study were not able to resolve the lowest two classes (i.e., size classes only ranged from 0.312 to 24.5 mm). The class width is finer for smaller and medium-sized particles and broadens for larger particles (Table A1 in Yuter et al. 2006). The instrument accumulates the number of particles per diameter and fall velocity class over a predefined time resolution ranging from 10 to 3600 s. A detailed description

and specifications of the instrument’s hardware and data analysis are found in Löffler-Mang and Joss (2000), Löffler-Mang and Blahak (2001), Yuter et al. (2006), and references within. A short description of the calculation of the moments of the DSD can be found in appendix A. For strong rain and for rain with a large number of drops a correction function is also applied, which calculates the estimated real number concentration (Raasch and Umhauer 1984). Löffler-Mang and Joss (2000) estimated the probabilities of coincidence to be about 5% for an extreme convective shower (with size distribution parameter  $N_0 = 1400 \text{ m}^{-3} \text{ mm}^{-1}$  and rain rate of 300 mm h<sup>-1</sup>) and 10%

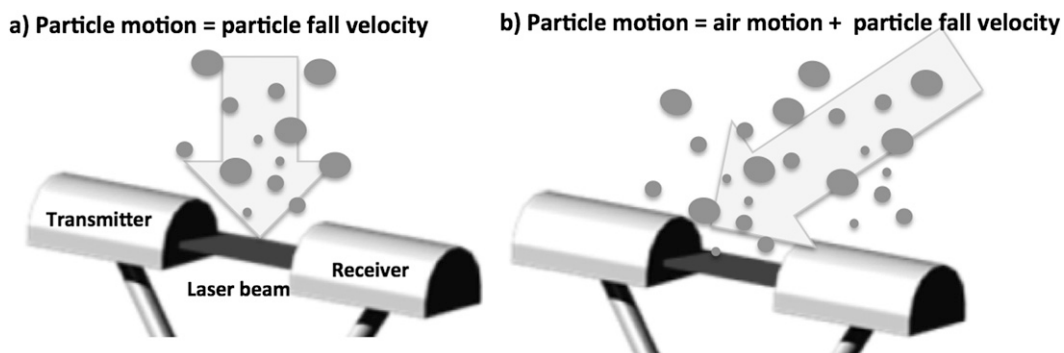


FIG. 2. Schematic showing the measurement principle of a PARSIVEL disdrometer under (a) no wind and (b) windy conditions. In (a), particle motion is equal to the fall velocity when there is no air motion. The particle motion is indicated by gray arrow; particles are indicated by gray filled circles. In (b), during windy conditions, particle motion is the sum of air motion and the particle fall velocity. The measurement principle under no-wind conditions is schematically illustrated in Fig. 1 in Löffler-Mang and Joss (2000).

for strong stratiform rain ( $N_0 = 8000 \text{ m}^{-3} \text{ mm}^{-1}$  and rain rate of  $100 \text{ mm h}^{-1}$ ).

### b. Articulating disdrometers

In the presence of wind, a particle trajectory deviates from the vertical terminal fall track to a slanted track (Fig. 2b). The particle motion is dependent on gravitational forces and wind-induced drag forces arising from the difference between air motion and the speed of the particle. To improve measurement accuracy in strong winds, several studies have suggested orienting the disdrometer sampling area perpendicular to the wind direction (Bradley and Stow 1975; Griffiths 1975). The University of Florida (UF) designed an “articulating” disdrometer system that continuously aligns the disdrometer sampling area with the mean 10-s particle trajectory, such that the measurement plane is perpendicular to the particle motion in an averaged sense (Fig. 1b; Lopez et al. 2011; Friedrich et al. 2013). A PARSIVEL disdrometer and an RM Young model 85106 2D sonic anemometer are mounted on an actively controlled platform that continuously changes the azimuth and elevation angles of the disdrometer to orient the sampling area semiperpendicular to the particle motion. The azimuth setpoint corresponds to the 10-s moving average of the wind direction. The elevation angle setpoint corresponds to the inverse arctangent of the 10-s moving average of the horizontal wind speed and the mean particle fall velocity; a particle fall velocity of  $4.5 \text{ m s}^{-1}$  ( $d = 1.2 \text{ mm}$ ) was assumed for the articulating disdrometer. The articulating disdrometers were first deployed and tested during VORTEX2 in 2010; no measurements of articulating disdrometers are available for Hurricane Ike in 2008. A detailed description of the fall velocity correction for articulating disdrometers can be found in Friedrich et al. (2013).

## 3. DSD measurements in strong winds and heavy rainfall

### a. Hurricane Ike

Two stationary PARSIVEL disdrometers (denoted as CU01 and CU02) were deployed approximately 3 and 6 km, respectively, from the Galveston Island coastline in Texas during the landfall of Hurricane Ike on 12–13 September 2008 (Fig. 3a). A Droplet Measurement Technologies precipitation imaging probe (PIP; a detailed description is available at <http://www.dropletmeasurement.com>) was deployed by the University of Florida about 30 km north of Galveston Island (Fig. 4a). Hurricane Ike was a category 2 hurricane on the Saffir–Simpson Hurricane Wind Scale (Simpson 1974; Saffir 1975) at

landfall, with wind speeds of about  $49 \text{ m s}^{-1}$  and a central pressure of about 950 mb (Berg 2009). Most of south-eastern Texas received more than 8 cm of total rainfall from Hurricane Ike, with a maximum of 25 cm of total rainfall around Houston, Texas (Berg 2009). During landfall the hurricane moved toward the north-northwest.

Disdrometer measurements and surface observations of wind, temperature, and humidity were taken during the rainfall associated with the landfall of Hurricane Ike. Observations were recorded between 2200 UTC 12 September 2008 and 1400 UTC 13 September 2008 covering the outer and inner hurricane rainbands, the eyewall area, and the eye of the hurricane as illustrated in Fig. 3b. The long axis of the stationary disdrometer sampling area was oriented perpendicular to the wind (i.e., the instruments were oriented northwest–southeast) and measurements were accumulated over 1-min intervals. During the observation period the wind speed increased steadily over 8 h from  $15$  to  $27 \text{ m s}^{-1}$  on the north side of the hurricane. After the hurricane eye passed over the instruments, the wind speed decreased from  $25$  to  $15 \text{ m s}^{-1}$  over the next 5 h (Figs. 3c,d). Wind speeds were slightly stronger at CU01, which was located approximately 4 km closer to the Galveston Island coast line. Wind direction changed from north to northeast on the northern side and southwest to west on the southern side of the storm. Similar wind patterns but with lower wind speeds were also observed farther inland at the location of the PIP (Fig. 4b).

The drop size distributions measured by the two stationary PARSIVEL disdrometers clearly show an overestimation of the number concentration of medium-sized ( $d \sim 2\text{--}4 \text{ mm}$ ) and large drops ( $d > 4 \text{ mm}$ ) over almost the entire sampling period (Figs. 3c,d). In comparison, the PIP observed mainly raindrops with  $d < 3 \text{ mm}$  and only occasionally large-sized raindrops with  $d \sim 3\text{--}5 \text{ mm}$  with a much lower number concentration (Fig. 4b). Note that the PIP only measures particles with sizes from 0.1 to 6.2 mm and has a sampling area ( $26 \times 0.62 \text{ cm}^2$ ), which is almost 3.5 times smaller than the PARSIVEL sampling area ( $3 \times 18 \text{ cm}^2$ ). Previous studies using ground-based and airborne disdrometers in tropical cyclones and hurricanes indicate a high concentration of small and medium-sized drops ( $d < 4 \text{ mm}$ ) with the absence of larger drops (e.g., Merceret 1974a,b; Jorgensen and Willis 1982; Wilson and Pollock 1974; Ulbrich and Lee 2002; McFarquhar and Black 2004; Maeso et al. 2005). Tokay et al. (2008) present a comprehensive study of drop size distribution using several impact-type Joss–Waldvogel disdrometers in seven tropical cyclones between 2004 and 2006. They observed a maximum drop diameter during these storms of 4 mm and mean mass diameter of 1.7 mm while the maximum

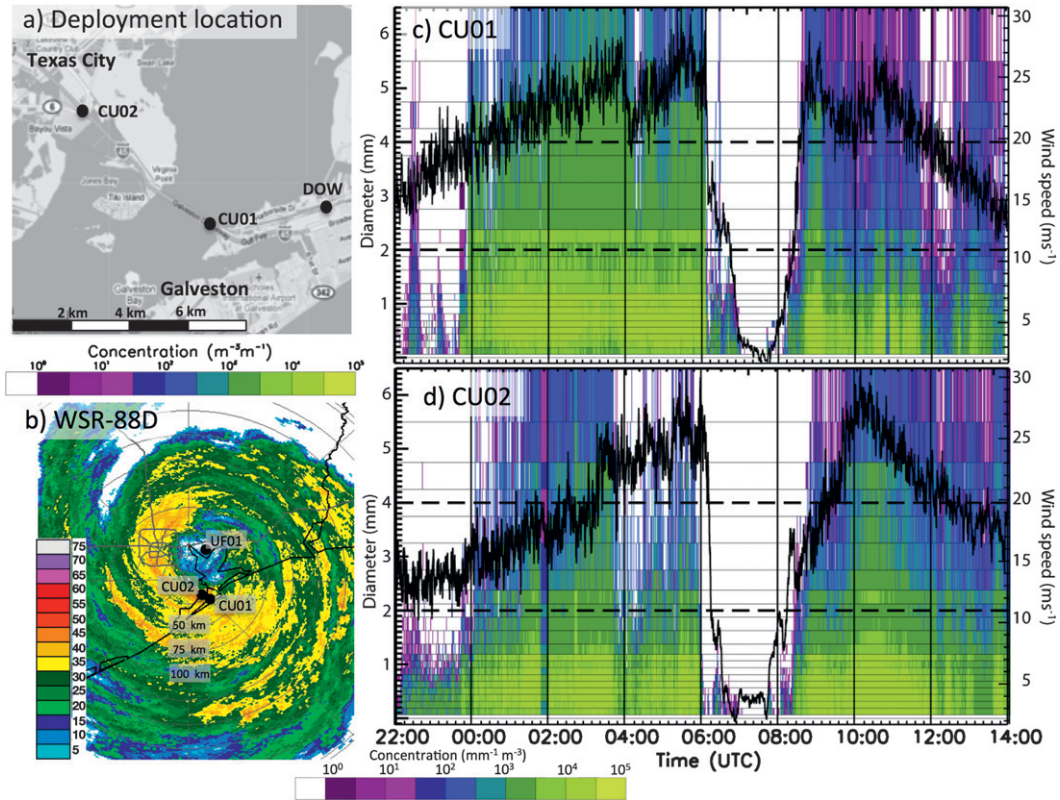


FIG. 3. Measurements during the landfall of Hurricane Ike on 12–13 Sep 2008 at Galveston, TX. (a) Location of disdrometers CU01 and CU02 and the DOW radar (source: Google maps). (b) Radar reflectivity (dBZ) from the Weather Surveillance Radar-1988 Doppler (WSR-88D) in Houston, TX, observed at 0900 UTC 13 Sep. Black lines present state borders and thick gray lines indicate highways. Range rings are centered at the radar location and are indicated every 25 km. The locations of the disdrometers are indicated as filled circles. Number concentrations per unit volume (color coded) as a function of diameter class and time measured by the stationary disdrometer (c) CU01 and (d) CU02 accumulated over 1 min. Wind observations at 1 Hz at the disdrometer location are indicated as solid black lines in (c) and (d). Diameter classes are indicated by thin black lines; 2- and 4-mm diameters are highlighted by thick dashed lines.

wind speed ranged between 7 and 13  $\text{m s}^{-1}$ . Although drops with diameters larger than 5–5.5 mm cannot be distinguished by the Joss–Waldvogel disdrometer (Tokay et al. 2005), the two-dimensional video disdrometer also supports the presence of drops with mean mass diameters of 1–1.4 mm in tropical cyclones (Maeso et al. 2005). The drop size distributions measured by the stationary disdrometers CU01 and CU02 deployed close to Galveston Island during Hurricane Ike do not resemble anything that has been reported in the literature to date, although we note that the Tokay et al. (2008) study intentionally removed measurements during strong winds. The overestimation of large drops by the stationary disdrometer decreased when the wind speed decreased after 1000 UTC 13 September 2008. The DSD observed by the PIP with particle diameters mostly below 3–4 mm resamples DSD measurements (number concentration and particle sizes) in hurricanes or tropical cyclones from previous

studies. The difference in drop-size concentration between the northern and southern side of the hurricane at times when similar wind speeds were observed can be related to differences in rainfall rate.

The fall velocity–diameter histograms for two individual time steps show an unrealistic relationship between fall velocity and diameter for the stationary disdrometer CU01 (Figs. 5a,b). A large number of raindrops were misclassified as large raindrops ( $d > 4$  mm) with low fall velocities  $< 2 \text{ m s}^{-1}$ . Based on laboratory and field experiments, the fall velocity–diameter histogram should be aligned closely to the average fall velocity–diameter relation for rain described in Gunn and Kinzer (1949) and Atlas et al. (1973) and as shown by the solid black line in Fig. 5. Note that the stationary instruments also observed spurious raindrops, which may be caused by raindrops splashing on the instruments and raindrops falling through the edges of the

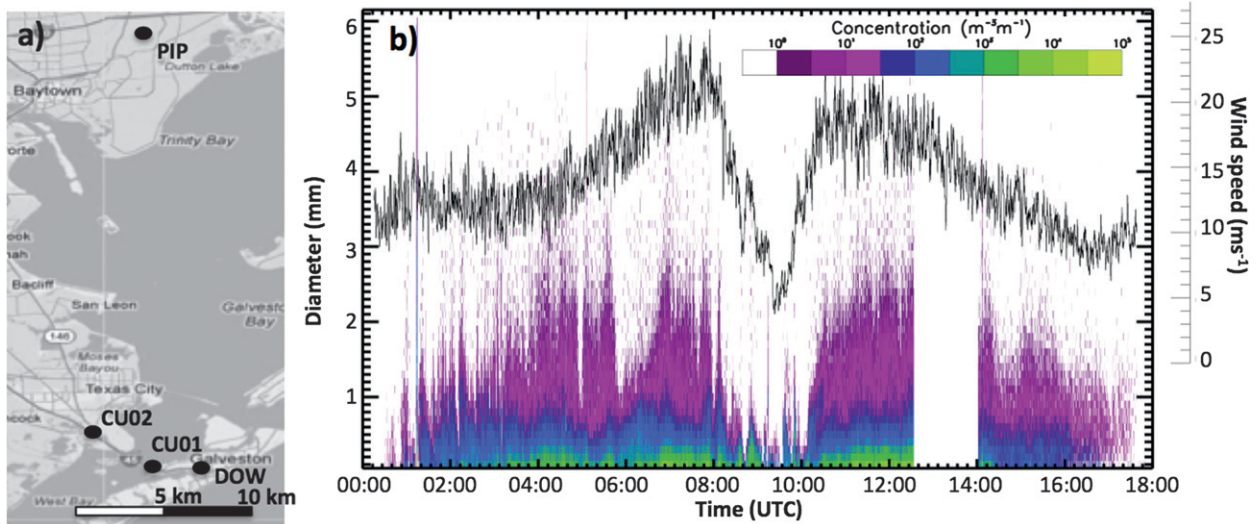


FIG. 4. Measurements during the landfall of Hurricane Ike on 12–13 Sep 2008 approximately 30 km north of Galveston, TX. (a) Location of PIP probe, disdrometers CU01 and CU02, and the DOW radar (source: Google maps). (b) PSD from the PIP every 10 s overlaid by wind speed measurements. Note that no data were recorded between 1300 and 1400 UTC by the PIP.

laser. These “splashing” and “margin faller” effects are discussed in more detail in appendix B.

#### b. Supercell thunderstorms during VORTEX2

During the VORTEX2 campaign, two articulating and six stationary mobile disdrometers were deployed within 36 thunderstorms resulting in over 250 cross-section measurements (Friedrich et al. 2013). Two of the stationary mobile disdrometers were CU01 and CU02, the same disdrometers that were deployed in Hurricane Ike. VORTEX2 was conducted for a total of 12 weeks between 11 May and 14 June 2009 and between 3 May and 14 June 2010. Contrary to the procedure during Hurricane

Ike, the sampling interval was set to 10 s for all instruments so that the wind artifact observed during Hurricane Ike could be removed without losing minutes of observations.

Precipitation particles observed at the surface in supercell thunderstorms generally consist of rain, graupel, small ice particles, and small hailstones that we will refer to as PSD hereafter. Figure 6 shows the number concentrations collected by a stationary disdrometer during one of the VORTEX2 deployments. Note that no quality control has been applied to the data. Unrealistically high concentrations, similar to those observed during Hurricane Ike, were observed between 2305 and 2314 UTC 13 June 2010 when wind speed

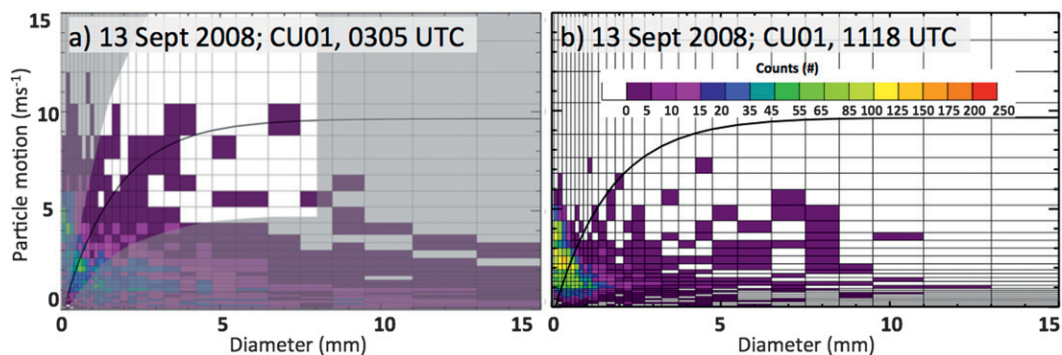


FIG. 5. Fall velocity–diameter histograms observed on 13 Sep 2008 at (a) 0305 and (b) 1118 UTC during the landfall of Hurricane Ike. Number of drops (raw counts; color coded) accumulated over 1 min is plotted as a function of particle motion and particle diameter. Thin black lines represent the particle size and velocity classes. Solid black line indicates the empirical fall velocity–diameter relation for rain described in Atlas et al. (1973). Gray shading in (a) indicates the particles that are removed because they are above or below 50% of the fall velocity–diameter relation for rain.

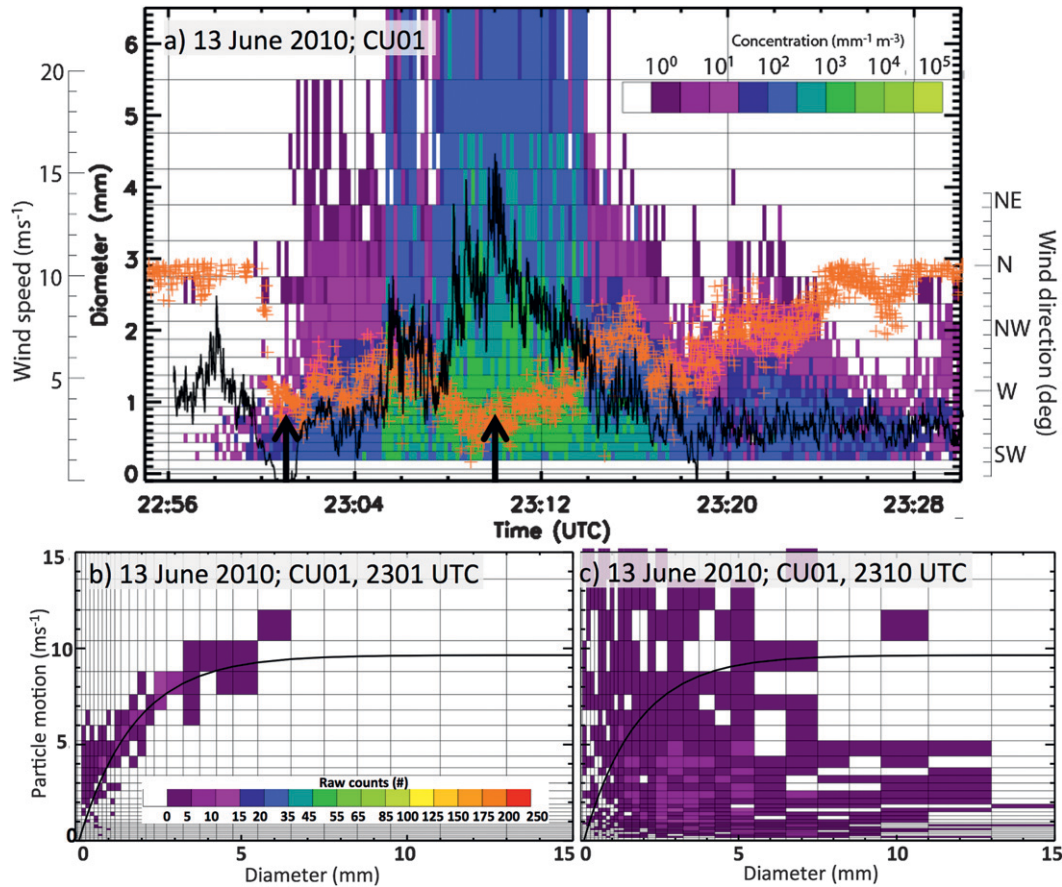


FIG. 6. (a) Time series of number concentrations per unit volume (color coded) as a function of diameter class and time measured by the stationary PARSIVEL disdrometer on 13 Jun 2010 during VORTEX2. Number concentrations are plotted based on the sampling interval of 10 s. Thick black line and orange plus symbols indicate wind speed and wind direction every 1 s, respectively. (b),(c) As in Fig. 5, but for raw counts measured at 2301 and 2310 UTC 13 Jun 2010, respectively. Times are indicated by black arrows in (a).

exceeded  $7 \text{ m s}^{-1}$  (Fig. 6a). The fall velocity–diameter histogram at 2310 UTC (Fig. 6c), also collected by a stationary disdrometer, shows a similar pattern to the histograms measured during Hurricane Ike (Fig. 5). The histograms during strong winds ( $>7 \text{ m s}^{-1}$ ) are characterized by large particles with  $d > 6 \text{ mm}$  and low particle velocities ( $<3 \text{ m s}^{-1}$ ). When the wind velocities decrease to below  $5 \text{ m s}^{-1}$  at 2301 UTC the number concentrations line up with the fall–velocity–diameter relation (Fig. 6b). In addition to wind speed, the wind direction relative to the orientation of the instruments may also affect measurement quality. The manufacturer recommends deploying the instrument with its long axis perpendicular to the wind. The instrument was deployed in an east–west direction with the sampling area perpendicular to the northerly wind at the beginning of the deployment. After 2300 UTC, the wind backed to  $230^\circ$ – $300^\circ$ . In other words, the offset between wind direction

and the disdrometer sampling area, which is ideally  $90^\circ$ , decreased to  $30^\circ$ – $40^\circ$  after 2300 UTC. Note that the large slowly falling particles do not resemble typical fall velocity–diameter relationships of ice particles (see appendix B and Fig. B1). Since the wind speed increases only temporarily in supercell thunderstorms compared to steady strong winds in hurricanes, the ambiguous number concentrations were observed for a few seconds and occurred far less often than in Hurricane Ike. The longest occurrence of ambiguous drops ( $\sim 8 \text{ min}$ ) out of 250 thunderstorms observed during VORTEX2 is presented in Fig. 6. The articulating disdrometers were not deployed on 13 June 2010.

Interestingly, the large slow-falling drops (denoted as wind effect hereafter) were never observed by the articulating disdrometers during VORTEX2. Therefore, we can hypothesize that the spurious particles observed by the stationary disdrometers are related to

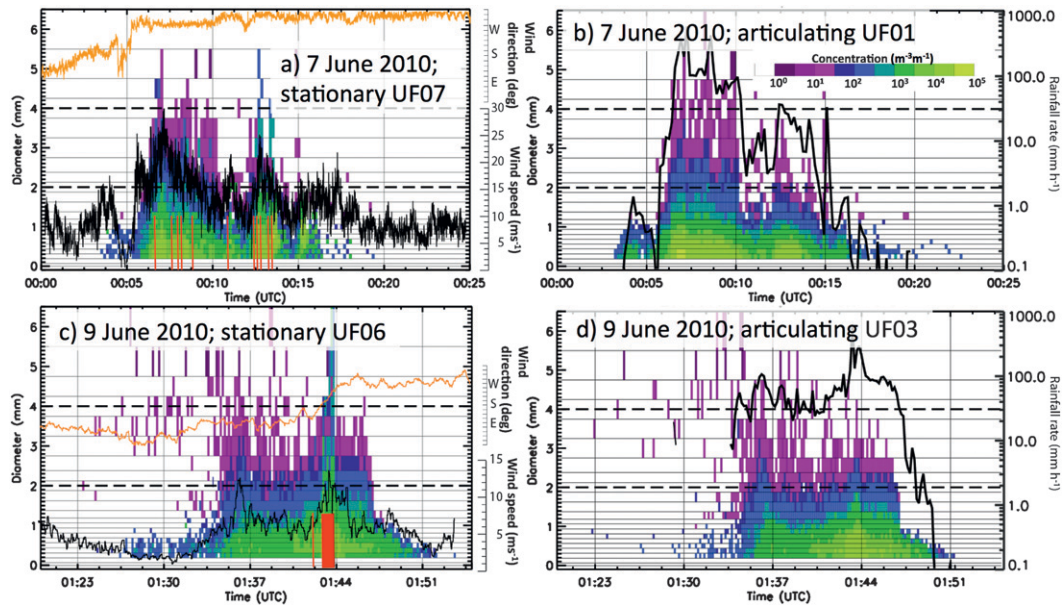


FIG. 7. As in Fig. 6a, but showing number concentration per unit volume (color coded) for collocated (a),(c) stationary and (b),(d) articulating disdrometer measurements conducted on 7 Jun 2010 and 9 Jun 2010 during VORTEX2. In (a),(c), solid black and orange lines indicate wind speed and wind direction at 1 Hz, respectively; red lines indicate the times when spurious particles were observed by the stationary disdrometer. In (b),(d), solid black lines show rainfall rate measured by the articulating disdrometer.

particles falling at an angle through the sampling area. Figure 7 shows collocated PSD observations from a stationary disdrometer (Figs. 7a,c) compared to observations from the articulating disdrometer (Figs. 7b,d) in two supercell thunderstorms on 7 and 9 June 2010 during VORTEX2. The maximum wind speed was  $27 \text{ m s}^{-1}$  on 7 June and  $14 \text{ m s}^{-1}$  on 9 June. Ambiguous large-diameter drops occurred occasionally between 0006 and 0014 UTC 7 June when the wind speed ranged from 15 to  $27 \text{ m s}^{-1}$ . High number concentrations were observed at 0143–0144 UTC 9 June when winds speeds exceeded  $7 \text{ m s}^{-1}$ . On both days, wind encountered the disdrometer sampling area at an angle of about  $60^\circ$ – $75^\circ$  (with  $90^\circ$  being optimal). The stationary disdrometer was oriented southwest–northeast on 7 June and north–south on 9 June. These time steps as indicated in Figs. 7a and 7c were identified based on the fall velocity–diameter histograms, which resemble those shown in Figs. 5 and 6c. It should be noted that high wind speed does not always lead to an ambiguous number concentration, as shown between 0006 and 0010 UTC 7 June when wind speeds and rainfall rates were high ( $>15 \text{ m s}^{-1}$ ;  $>100 \text{ mm h}^{-1}$ ). Earlier on 9 June at around 0135 UTC when the rainfall rate was approximately  $100 \text{ mm h}^{-1}$ , the wind reached a local maximum of  $12 \text{ m s}^{-1}$  but did not cause ambiguous large drops to occur. It can only be hypothesized that wind direction or turbulence

effects suppressed the wind effects during strong winds on 7 and 9 June 2010.

#### 4. Discussion

##### a. Comparing stationary disdrometers with Doppler radar during Hurricane Ike

In the first part of the discussion, we will investigate whether spurious raindrops can be removed with a simple quality-control scheme and how the spurious raindrops affect the DSD and comparisons with radar reflectivity. First, we will only use measurements that are 25%–75% above or below the typical fall velocity–diameter relationship for rain, removing most of the spurious drops. Jaffrain and Berne (2011) compared 15 months of rain gauge and PARSIVEL disdrometer measurements and concluded that excluding data that are more than 60% above or below the fall velocity–diameter relationship for rain will give a good agreement (3.5% differences of total rain amount) between PARSIVEL disdrometers and rain gauges. Other studies use a threshold of 40% above or below the fall velocity–diameter relationship for rain to remove misclassified drops (Kruger and Krajewski 2002; Thurai and Bringi 2005). However, these studies do not discuss the influence of wind on the measurement accuracy.

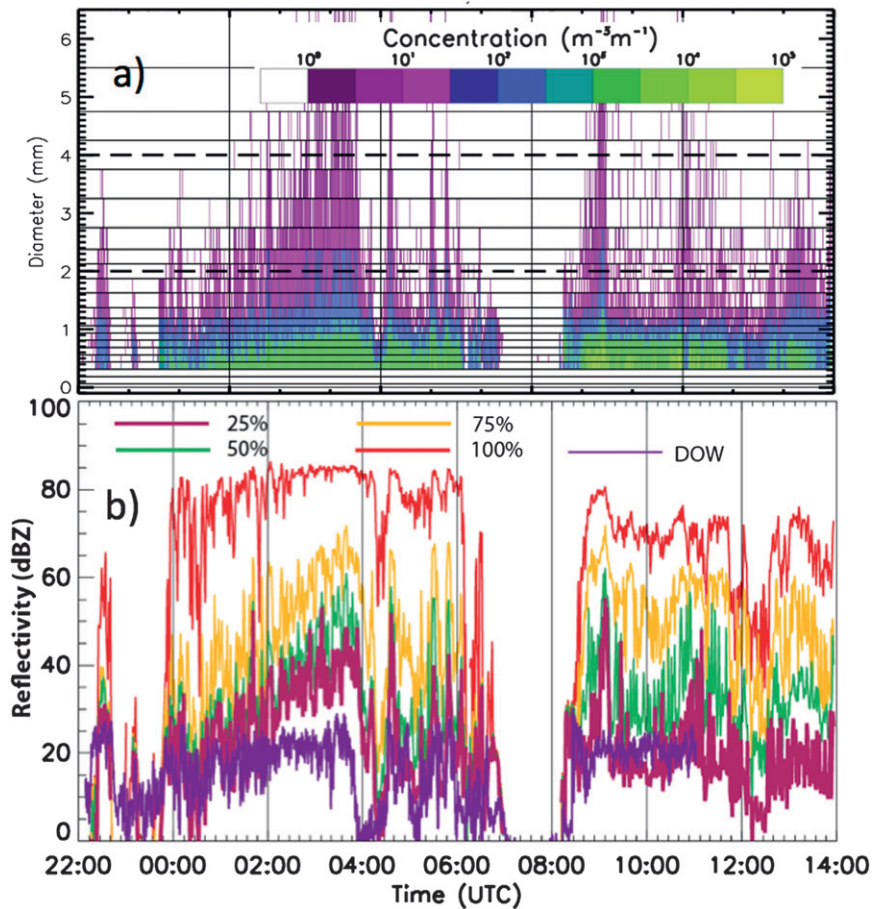


FIG. 8. (a) As in Fig. 3c, but only considering drops within  $\pm 50\%$  of the average fall velocity–diameter relation for rain. (b) Time series of reflectivity based on no quality control (red line), only considering drops that are  $\pm 25\%$  (dark red line),  $\pm 50\%$  (green line), and  $\pm 75\%$  (yellow line) of the rain–velocity line, and measured by the DOW radar (purple line).

Since drops are canted and distorted in strong winds, the shape and oscillation characteristics may differ from low wind conditions. The question remains whether we can remove the ambiguous drops and still maintain a representative DSD. As a first attempt, we removed all drops with  $d > 8$  mm and only considered those drops with particle motions that were within a certain percentage of the average fall velocity–diameter relation for rain (gray shading in Fig. 5a). When only drops that are within  $\pm 50\%$  of the fall velocity–diameter relationship are considered, as shown in Fig. 8a, the DSD is closer to those DSDs observed by the PIP and by Tokay et al. (2008) in hurricanes and tropical cyclones, where raindrop diameters were mostly below 4 mm. Reflectivity values based on the disdrometer measurements decrease significantly when only drops are considered that were classified into the velocity bins located within  $\pm 25\%$ – $75\%$  of the rain velocity line (Fig. 8b). By

doing so, a large number of drops are removed and the total number concentration decreases from  $>10^5 m^{-3}$  to  $10^3$ – $10^4 m^{-3}$  when only drops are used that are  $\pm 50\%$  of the rain line (figure not shown). For this dataset, the errors related to this approach are difficult to quantify because there is no reference measurement of DSD. However, the modified  $\pm 25\%$  disdrometer reflectivity values (dark red line in Fig. 8b) are the closest (with differences of 5–25 dB) to the reflectivity values observed by the Doppler on Wheels (DOW) X-band radar (purple line in Fig. 8b), which was located on Galveston Island (Fig. 3a) about 3 km east of CU01. Nevertheless, large differences of up to approximately 25 dB between 0200 and 0400 UTC show that the simple selection of drops along the fall velocity–diameter relationship lowers the reflectivity values but does not necessarily represent a reliable reflectivity evolution. On the other hand, radar reflectivity measured with X-band radar can

be heavily attenuated by large drops and heavy rainfall that occurs in hurricane rainbands. While the disdrometer reflectivity values between 2200 and 0000 UTC only show small differences below 5 dB, attenuation causes a drift in reflectivity differences up to 25 dB between 0000 and 0400 UTC.

Applying the  $\pm 40\%$ – $60\%$  thresholds based on the fall velocity–diameter relationship for rain will remove spurious drops most likely related to splashing and margin fallers from the disdrometer data and therefore improve any comparison of rainfall rate and accumulated rainfall between disdrometers and rain gauges. So far, we cannot quantify the effects of removing spurious drops from the DSD during events with strong winds and heavy rainfall since the “true” DSD from another type of disdrometer collocated to the OTT PARSIVEL was not available during strong wind cases. In section 4b, we are using the articulating disdrometer in an attempt to quantify removal of spurious drops for a few minutes of collocated measurements in strong wind. In the future, a comparison experiment between the PARSIVEL and other types of disdrometers (e.g., 2D video disdrometer) might help quantify the effects. Until then, we would recommend that a terminal fall velocity threshold identifying the occurrence of large ( $d > 5$  mm), slow-falling ( $v < 1$  m s<sup>-1</sup>) particles should be included in the post processing that identifies times with mismatched drops based on the fall velocity–diameter histogram. If spurious particles are detected with the terminal fall velocity threshold, the time step should be removed completely from the analysis (see appendix B and Fig. B1). For the remainder of the paper, if the entire time step is removed, we refer to it as the terminal fall velocity threshold. If large slow-falling particles are not detected during the individual time steps, then the  $\pm 40\%$ – $60\%$  thresholds can be applied to the data (see appendix B and Fig. B1).

#### *b. Comparison between stationary and articulating disdrometer during strong winds*

Since the ambiguous drop concentrations were only observed in the stationary disdrometer measurements, it can be hypothesized that this artifact is related to the fact that particles move at an angle through the disdrometer sampling area. Moreover, particles might be canted and distorted in strong winds, which leads to misclassification in the diameter class especially for larger particles that will occur in both the stationary and articulating disdrometers. At this point, we cannot quantify the effects of canting and distortion. To further investigate the different effects of particle motion on measurements with stationary and articulating disdrometers and to validate the quality control discussed

in section 4a, individual 10-s time steps are compared from VORTEX2 collocated deployments (section 3b). We compare the time steps showing spurious data from the stationary disdrometer with the same time steps measured by the articulating disdrometer for 7 and 9 June (times are highlighted in Figs. 7a,c). Although the sampling error is relatively high for 10-s accumulation time based on the analysis by Jaffrein and Berne (2011), we decided not to average over larger time intervals in order to have enough samples to compare ambiguous and nonambiguous samples. Therefore, we focus solely on trends and relative values rather than absolute values. Figure 9 shows the differences in raw counts and radar reflectivity between the stationary and articulating disdrometer for the entire deployment on 7 and 9 June, respectively. The stationary disdrometer counted slightly more particles during calm conditions ( $< 5$  m s<sup>-1</sup>). The large variation for small numbers of raw counts ( $< 100$ ) during calm conditions is primarily related to the particles observed prior to 0134 UTC 9 June. With increasing wind speeds ( $5$ – $15$  m s<sup>-1</sup>) the articulating disdrometer counted more particles. The reflectivity is calculated at times when the maximum number of raw counts is larger than 1600 to avoid comparing data within weak showers (e.g., Fig. 8 prior to 0134 UTC). Furthermore, the maximum diameter is limited to 8 mm, which limits the analysis to raindrops, graupel, and tiny hailstones. Note that the appendix describes a particle dissemination algorithm, which we developed based on the VORTEX2 and hurricane data (Friedrich et al. 2013). In this comparison, we cannot apply the quality control described in appendix B because it would remove the spurious drops. During calm conditions ( $< 5$  m s<sup>-1</sup>) on 9 June, reflectivity values differ by 5–10 dB (pink triangle symbols in Fig. 9b) and spread farther apart with increasing wind speed. The large differences in calm conditions occur mainly at the edge of the thunderstorm (0125–0132 UTC in Figs. 7c,d) with differences in the medium-sized particles ( $d \sim 3$ – $5$  mm), which strongly affect the reflectivity values. For wind speeds  $> 10$  m s<sup>-1</sup>, the stationary disdrometer measures larger reflectivity values for the vast majority of the PSD spectra observed on 7 and 9 June. Since reflectivity is a function of the 6th power of drop diameter, larger particles have a stronger influence on the reflectivity value compared to smaller drops. After removing the ambiguous particles (particles outside the  $\pm 25\%$  fall velocity–diameter relationship), the number of larger particles ( $d > 2.5$  mm) decreases (Fig. 9c), resulting in a decrease in reflectivity and a decrease in spread (difference between the 16th and 84th percentile) between the reflectivity values of the stationary and articulating disdrometer (Fig. 9d). At the same time, the number of raw particles counted by

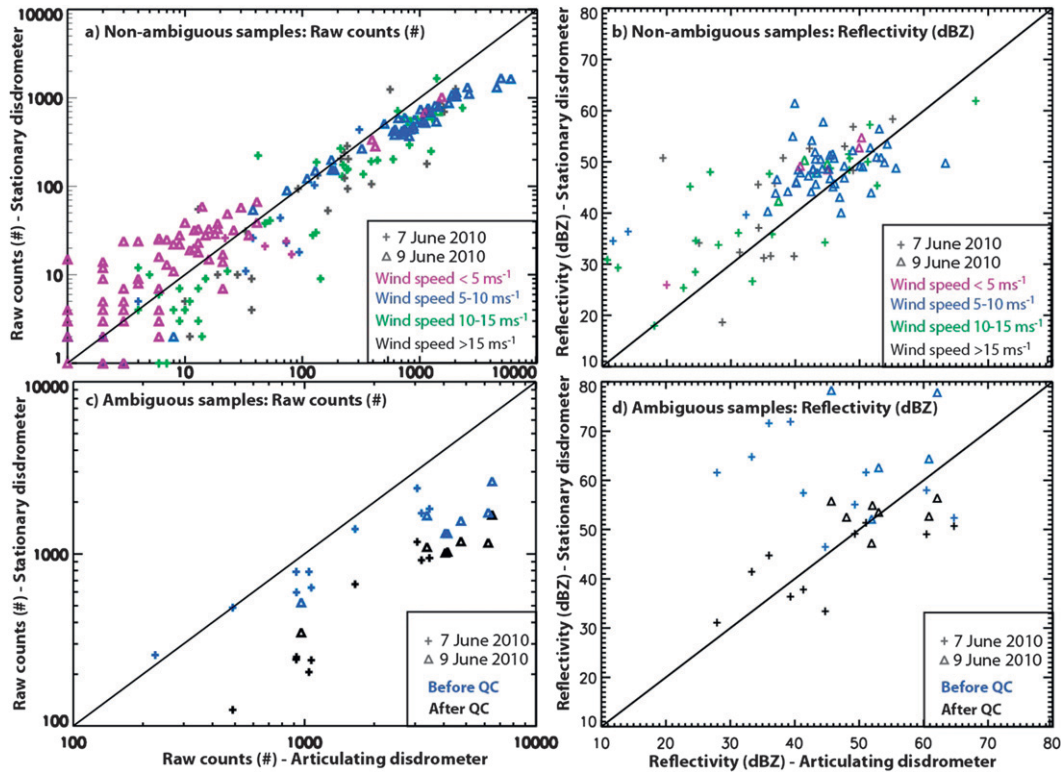


FIG. 9. Comparison between articulating and stationary disdrometers for measurements conducted on 7 Jun 2010 (triangle symbols represent articulating disdrometer, UF01, and stationary disdrometer, UF07) and 9 Jun 2010 (plus symbols represent articulating disdrometer, UF03, and stationary disdrometer, UF06). (a) Total number concentration and (b) reflectivity for all time steps without ambiguous measurements. Wind speed observations from the anemometer are color coded. (c) Total number concentration and (d) reflectivity for time steps with ambiguous measurements. Each symbol represents 10-s accumulation interval.

the stationary disdrometer decreases (black symbols in Fig. 9c) compared to the articulating disdrometer. While some decrease in particle counts is associated with the removal of large drops, the majority of drops that are removed have  $d < 2 \text{ mm}$  as indicated in Fig. 10. Note that errors in reflectivity can also be related to the sampling interval. Jaffrein and Berne (2011) determined a sampling uncertainty for radar reflectivity of less than 15% for 1-min sampling intervals. This analysis shows that the reduction of larger drops might lead to a more realistic reflectivity value, but not necessarily to a more realistic particle size distribution (Fig. 10). We can assume that the articulating disdrometer is less affected by wind and therefore shows more reliable number counts compared to the stationary disdrometer. Figures 9 and 10 show that simply using the measurements close to the fall velocity–diameter relationship is not justified when misclassified particles are observed. It does lower the reflectivity values similar to those observed by the articulating disdrometer (Fig. 9d), but it also changes the DSD and reduces the number of counts to values much

lower than those observed by the articulating disdrometer (Figs. 9c, 10). As a result, we would recommend completely removing time steps when the terminal fall velocity threshold applies, that is, when the fall velocity–diameter histogram shows large particles ( $d > 5 \text{ mm}$ ) with low fall velocity ( $v < 1 \text{ m s}^{-1}$ ).

*c. Comparison between stationary and articulating disdrometer during VORTEX2*

Stationary and articulating disdrometers were occasionally collocated during VORTEX2 to estimate the differences in reflectivity, total number concentration, and composite DSD between these two types of instruments. Measurements were conducted in five thunderstorms (~2 h) and differences are shown in Figs. 11 and 12. Large differences between the stationary and articulating disdrometers occurred in the non-quality-controlled reflectivity and number concentration fields with larger differences being observed for low number concentrations (Fig. 10e;  $N_T < 1000 \text{ m}^{-3}$ ). Splashing and margin faller effects identified by the particle discrimination

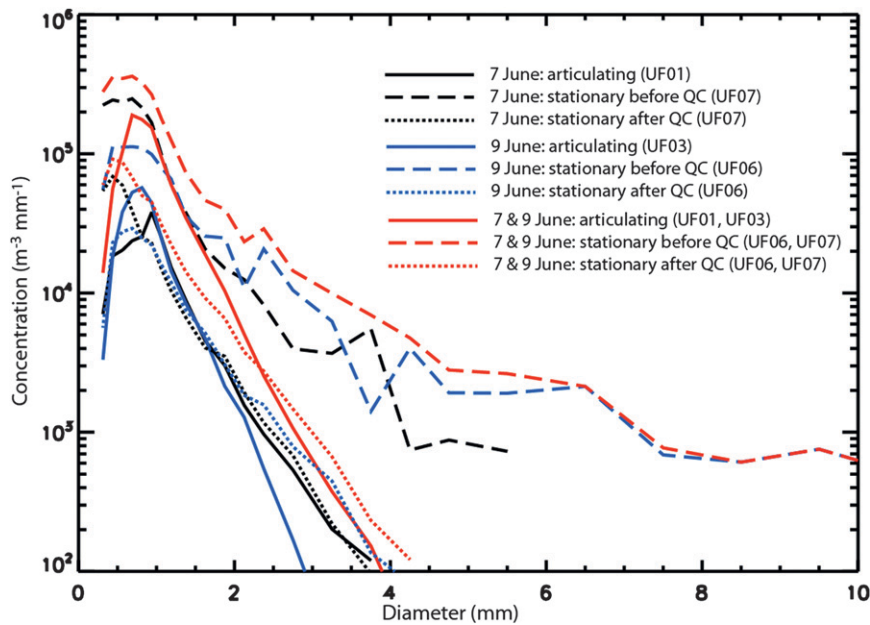


FIG. 10. Composite particle size distributions for the ambiguous samples shown in Figs. 9c,d including data from 7 Jun 2010 (black lines, 10 samples), 9 Jun 2010 (blue lines, 7 samples), and the composite data from both cases (red lines, 17 samples).

method described in appendix B primarily occurred when reflectivity values were  $<40$  dBZ in both instruments (Figs. 11a,c). Hail with  $d > 8$  mm (using the particle discrimination method) and wind effects (identified by the terminal fall velocity threshold) were observed when reflectivity values exceeded 40 dBZ (Figs. 11a,c). The distinction between rainfall rate from the articulating disdrometer (Figs. 11a,b) and wind speed (Figs. 11c,d) reveals that wind effects occur either at low rainfall rates ( $<40$  mm  $\text{h}^{-1}$ ) and high wind speed ( $>20$   $\text{m s}^{-1}$ ) or at high rainfall rates ( $>80$  mm  $\text{h}^{-1}$ ) and low wind speed ( $<10$   $\text{m s}^{-1}$ ). A quality-control procedure was applied including the terminal fall velocity threshold (removing time steps when particles are observed with  $d > 5$  mm and  $v < 1$   $\text{m s}^{-1}$ ) and the particle discrimination method (appendix B; Friedrich et al. 2013). Results are shown in Figs. 11b, 11d, and 11f. The median difference (articulating – stationary disdrometer) and spread difference in reflectivity changed from  $-1.4$  to  $1.29$  dB and from 12 to 8.5 dB, respectively. Larger reflectivity differences between the articulating and stationary disdrometer were observed for large reflectivity values ( $>40$  dBZ) without showing any correlation to wind speed (Fig. 11d). The difference in number concentration between the articulating and stationary instruments was characterized by a median of 48 particles  $\text{m}^{-3}$  and a spread of 4143 particles  $\text{m}^{-3}$  after quality control was applied (Fig. 11f). Higher number concentrations were observed for stronger winds within the thunderstorms sampled during VORTEX2.

The composite quality-controlled DSDs for the five thunderstorm cases are subdivided into DSDs observed when the wind speed was  $<10$   $\text{m s}^{-1}$  (685 samples) and above  $10$   $\text{m s}^{-1}$  (80 samples) as indicated in Fig. 12. Small variations between the articulating and stationary disdrometer were observed for small drops ( $d < 2$  mm). The articulating disdrometer observes a higher concentration ( $200$ – $500$   $\text{m}^{-3} \text{mm}^{-1}$ ) of large drops ( $d > 5$  mm) and a higher concentration ( $500$ – $3000$   $\text{m}^{-3} \text{mm}^{-1}$ ) of medium-sized drops ( $2 < d < 5$  mm) compared to the stationary disdrometer. The differences in concentration between the articulating and stationary disdrometers at wind speeds  $<10$   $\text{m s}^{-1}$  are similar to the differences at  $>10$   $\text{m s}^{-1}$ . Note that measurements conducted in thunderstorms are usually characterized by a large spatial variation in DSD and that the comparison only includes approximately 2 h of observations. Further comparison between the two instrument types in more stratiform precipitation with lower variation in DSD needs to be conducted to validate the differences between the two instrument types.

#### d. Tilting experiment

In this simple experiment, the effects on the measured PSD from drops falling at different angles through the sampling area were investigated. The PARSIVEL disdrometer was set up in a laboratory while rainfall was simulated by dripping small droplets into the sampling area from a platform that was located about 4 m above

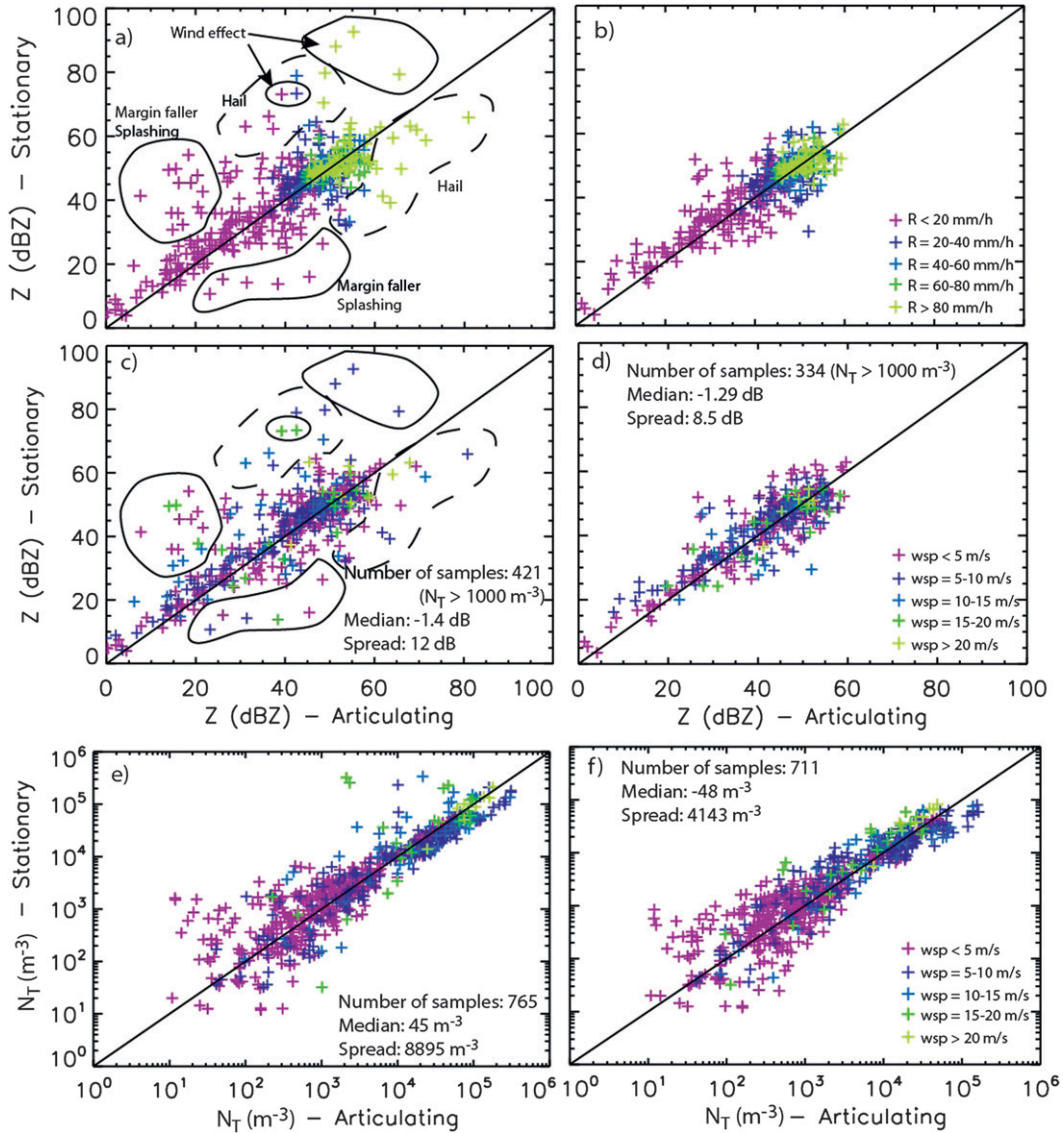


FIG. 11. Comparison between articulating and stationary disdrometers showing (a)–(d) reflectivity and (e),(f) total number concentration (left) before and (right) after a quality-control procedure was applied. Colors indicate various rainfall rates in (a),(b) and wind speeds in (c)–(f) measured by the articulating disdrometers. Number of samples, median, and spread (articulating – stationary) are indicated.

the instruments (top left, Fig. 13). The sampling interval was 30 s, during which approximately 30–40 drops were generated using a syringe (Fig. 13). This experiment was repeated 10 times and the drop counts were accumulated over 5 min (10 experiments × 30-s sampling interval). Drops generated by this method had diameters ranging between 0.8 and 4.5 mm. However, the distance between the syringe and the instrument was not large enough for the drops to reach terminal fall velocity (Fig. 13a). In an experimental study, Wang and Pruppacher (1977) showed that drops with diameters of 0.8–4.5 mm need at least 10 m to accelerate to terminal fall velocity.

The experiment was repeated tilting the instrument to 13°, 22°, 37°, and 45° (Figs. 13b–e). The fall velocity–diameter histogram of the 13°- and 22°-tilt experiment resembled the experiment with a horizontal sampling area. Increased splashing (indicated by small diameter drops with large fall velocity) is observed only with increasing instrument tilt (Figs. 13a–c). At 37° and larger (Figs. 13d,e), the measured fall velocity decreases for drops with a diameter between 2 and 6 mm, larger drops ( $d > 4.5$  mm) are observed, and splashing increases. Figure 13 shows the results when the instrument was tilted along its short axis. The experiment was conducted

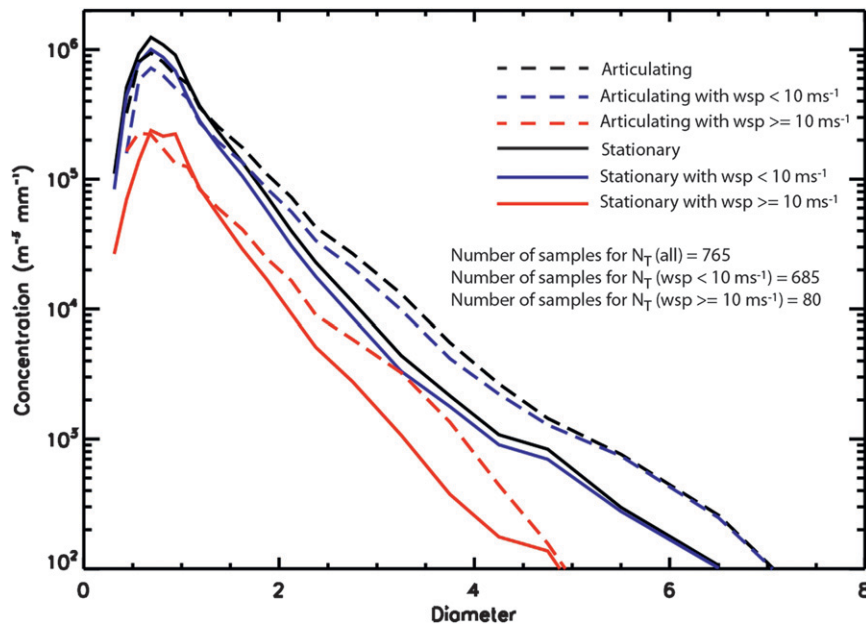


FIG. 12. Composite drop size distributions for all data (black lines) and data when the wind speed was below  $10 \text{ m s}^{-1}$  (blue lines) and above  $10 \text{ m s}^{-1}$  (red lines). Solid lines represent the DSD measured by the stationary disdrometer and dashed lines represent the measurements from the articulating disdrometer.

by tilting the instrument along both its long and short axis. However, tilting the instrument along its long axis reduces the size of the sampling area (e.g., for a  $45^\circ$  angle the width of the sampling area would reduce to 12.7 mm) and makes it less likely for drops to pass through the entire sampling area. The results of both experiments are similar, although the number of drops for the long-axis tilt experiment is much lower. The manufacturer recommends deploying the instrument with its long axis perpendicular to the wind.

## 5. Summary and conclusions

We examined the misclassification of particles by OTT PARSIVEL disdrometers deployed in Hurricane Ike 2008 and convective thunderstorms during VORTEX2 2010, characterized by a large number concentration of raindrops with large diameters ( $>5 \text{ mm}$ ) and unrealistically low fall velocities ( $<1\text{--}2 \text{ m s}^{-1}$ ). The investigation focused on two main issues: 1) analyzing the environmental conditions under which the misclassification occurs, and 2) discussing ways to minimize misclassification and treat misclassification in data postprocessing.

The misclassification was primarily observed by different stationary disdrometers at high wind speed and/or heavy rainfall. During Hurricane Ike, the misclassification was continuously observed during sustained winds

$>15 \text{ m s}^{-1}$  and reflectivity values  $<40 \text{ dBZ}$ . Even though wind speeds of more than  $10 \text{ m s}^{-1}$  were observed during most VORTEX2 deployments, the misclassification only occurred occasionally and only for few minutes in the stationary disdrometers. This would suggest that not only the wind speed but also the wind direction, the spatial variation of DSD, and the rainfall rate might affect measurements. The impact of spatial variations of the DSD and rain intensity has not been addressed in this study but could also intensify or weaken the occurrence of ambiguous drops especially during moderate wind conditions. A comparison between the articulating and stationary disdrometers shows that the misclassification can also occur at heavy rainfall and low wind speed. Once the wind speed exceeded a critical value, approximately  $15\text{--}20 \text{ m s}^{-1}$  based on the observations during Hurricane Ike and VORTEX2, the stationary disdrometers continuously observed unrealistically large slow-falling drops as seen during Hurricane Ike.

We hypothesize that particles not falling perpendicularly through the disdrometer sampling area can be one reason for the misclassification. A laboratory experiment showed that when drops do not fall perpendicular to the sampling area, the concentration of larger drops ( $>3 \text{ mm}$ ) increased while the fall velocity decreased (i.e., the empirical fall velocity–diameter relation for rain does not apply). Furthermore, the large slow-falling drops were not observed by the collocated articulating

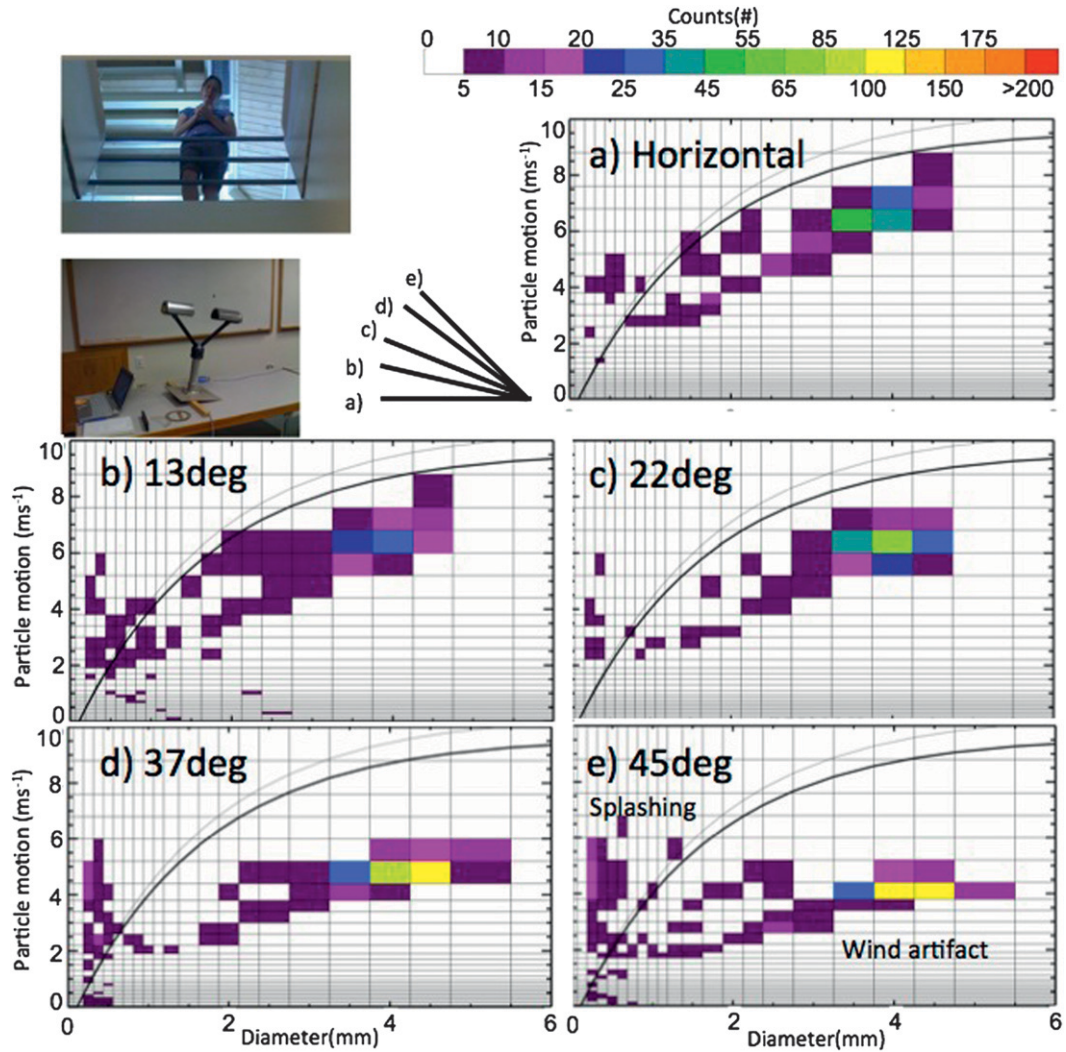


FIG. 13. (top left) Images showing the setup of the tilting experiment, in which drops generated about 4 m above the instrument were dripped into the PARSIVEL sampling area. Raw number counts (color coded) are illustrated for the instrument’s sampling area oriented (a) horizontally and tilted at (b) 13°, (c) 22°, (d) 37°, and (e) 45° along the short axis of the instrument. Drops were accumulated over 30 s, and each experiment was repeated 10 times. Black and gray lines indicate the diameter–velocity relationship (Gunn und Kinzer 1949; Atlas et al. 1973) at sea level and Boulder, CO (1663 m above sea level), respectively.

disdrometers. The correlation between disdrometer measurements and wind speed also indicates that the wind effect—although most likely present—does have a less noticeable effect when the wind speed is  $< 10 \text{ m s}^{-1}$ . Reflectivity values after removing the ambiguous counts, which are outside the  $\pm 25\%$  of the fall velocity–diameter relationship for rain, compare well with radar observations during Hurricane Ike and with observations from the articulating disdrometer operated during VORTEX2. On the other hand, the VORTEX2 dataset also indicates that the removal of larger drops provides similar reflectivity values for the stationary and articulating disdrometers, but also reduces the total number concentration

and changes the DSD in the stationary disdrometer compared to the articulating disdrometer. We are unable to determine whether the removal of the ambiguous counts produces a representative particle size distribution.

As a result, we recommend that, once the wind effect is observed in the data, those time steps should be completely removed using the terminal fall velocity threshold. When the instruments are deployed in conditions with strong winds (e.g., hurricanes), we recommend using articulating PARSIVEL disdrometers. Alternatively, windshields or fences commonly used for rain gauges (e.g., alter-type wind screens, double fence comparison reference, and rigid alter type) can be

placed around the disdrometer to minimize the influence of turbulence and wind speed [K. Nemeth, OTT, 2011, personal communication; R. Rasmussen, National Center for Atmospheric Research (NCAR), 2011, personal communication]. Comparison experiments in various terrain and climate regions showed that precipitation measured by rain gauges with windshields or fences increases by 20% for rain and 90% for snow (e.g., Weiss 1961; Brown and Peck 1962; Yang et al. 1998; Sugiura et al. 2006).

To better understand and quantify the effects of strong wind and heavy rainfall on the OTT PARSIVEL disdrometers, the instruments should be deployed with rain gauges and other disdrometer types such as 2D video disdrometer, precipitation imaging probe (PIP), and Joss–Waldvogel disdrometers with and without windshields or fences in conditions with strong wind and heavy rainfall. Although a large number of comparison studies have been conducted, these studies usually eliminate conditions of strong wind because of the poor performance of any rain-monitoring instrument. Although most manufacturers explicitly advise against the deployment in strong winds, our knowledge of microphysics in hurricanes and thunderstorms can only be broadened with a large set of in situ measurements at the surface. Although we cannot overcome the instrument limitations, we should be able to quantify the errors. We are currently comparing the performance of an articulating PARSIVEL disdrometer, a stationary PARSIVEL disdrometer, and a PIP at different wind speeds and rainfall rates in the University of Florida's Hurricane Simulator. In the simulator, wind speed, rainfall rate, and the orientation of the stationary disdrometer are modified. Further comparison studies under strong wind conditions are necessary to quantify the impacts of strong winds, varying wind directions, and rainfall rates on the performance of different types of disdrometers (e.g., PM-Tech PARSIVEL, 2D video disdrometer, articulating OTT PARSIVEL, and PIP) and to provide evidence for which disdrometer type is most suitable for strong wind conditions.

*Acknowledgments.* We extend special thanks to Rachel Humphrey, Danielle Nuding, Evan Kalina, George Fernandez, Scott Landolt, and Cameron Redwine who helped deploy the disdrometer during the VORTEX2 field campaign and Hurricane Ike deployment. Greatly appreciated is the help and advice of the four anonymous reviewers who significantly improved the quality of the paper. Our thanks go to Martin Hagen of Deutsches Zentrum für Luft- und Raumfahrt, David Kingsmill of CIRES/University of Colorado, and Sandra Yuter of University of North Carolina for many fruitful

discussions regarding this paper. We thank Karen Kosiba and Joshua Wurman of the Center for Severe Weather Research for providing the radar data for Hurricane Ike and Scott Kittelman and Samuel LeBlanc of University of Colorado for maintaining the instruments while installed at the ATOC Skywatch Observatory. We also thank Martin Löffler-Mang, Ulrich Blahak, Kurt Nemeth, and Eduardo Beck for clarifying some of the PARSIVEL internal data processing steps. This research was sponsored by the National Science Foundation under Grants ATM 0910424 (Friedrich) and AGS 0969172 (Friedrich). Stephanie Higgins was partially supported by the National Science Foundation Graduate Research Fellowship under Grant DGE 0707432. Any opinions, findings, and conclusions or recommendations expressed in this paper are those of the authors and do not necessarily reflect the views of the sponsors, partners, and contributors.

## APPENDIX A

### A Description of the Moments of the DSD

The PARSIVEL accumulates the number concentration of particles [denoted as  $n(D, v)_{ij}$ ] per diameter and fall velocity class over a predefined sampling time for each diameter size interval  $i$  and fall velocity interval  $j$ . After the quality control was applied to the number concentrations from the PARSIVEL disdrometer (raw counts), the number concentration  $n(D, v)_{ij}$  in each bin, which was measured over the sampling area of  $54 \text{ cm}^2$  using 32 velocity and 32 diameter classes, was converted to number concentration per unit volume of air:

$$N(D, v)_{ij} (\text{mm}^{-1} \text{m}^{-3}) = \sum_{i,j} \frac{10^6 n(D, v)_{ij}}{180 \text{ mm} (30 \text{ mm} - 0.5 D_i) v_j \Delta D_i \Delta t}. \quad (\text{A1})$$

Here,  $D_i$  (mm) is the  $i$ th mean diameter class,  $\Delta D_i$  (mm) is the width of the  $i$ th diameter class, and  $v_j$  ( $\text{m s}^{-1}$ ) is the  $j$ th mean velocity class. In 2009, the sampling interval  $\Delta t$  was set to 60 s. The temporal resolution was increased in 2010 ( $\Delta t$  was set to 10 s) to capture finescale variations in the observed PSDs. For each diameter class, number concentrations were summed over all of the velocity classes to determine  $N(D)_i$ . In the next step, the normalized number concentration within each diameter class was used to calculate reflectivity factor  $Z$  (dBZ) at a temporal resolution of 10 s (2010) or 60 s (2009) following Ulbrich (1983), Testud et al. (2001), Bringi et al. (2003), Yuter et al. (2006), and references within:

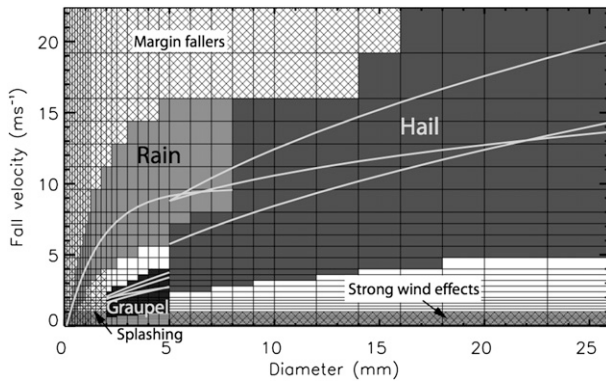


FIG. B1. Quality control developed based on Hurricane Ike and VORTEX2 data (Fig. 5a in Friedrich et al. 2013). Particle classification scheme based on typical diameter ranges and fall velocity–diameter relationships for rain (light gray-shaded boxes), hail (medium gray-shaded boxes), and graupel (dark gray-shaded boxes). Light gray lines indicate fall velocity–diameter relationships for rain, graupel, and hail, respectively. Time steps are completely removed if particles are observed with  $d < 5$  mm and  $v < 1$  m s<sup>−1</sup> (terminal fall velocity threshold).

$$Z(\text{dBZ}) = 10 \log_{10} \sum_i N(D)_i D_i^6 \Delta D_i. \quad (\text{A2})$$

## APPENDIX B

### Quality Control

A quality-control procedure was developed based on typical particle sizes and fall velocity–diameter relationships for rain, graupel, and hail (Fig. B1). The procedure is described in detail in Friedrich et al. (2013) and will only be summarized in this section. The quality control consists of removing the PSD of an entire time step if particles are observed with  $d > 5$  mm and  $v < 1$  m s<sup>−1</sup> (hatched area in Fig. B1, denoted as “wind effect” or terminal fall velocity method). It also includes a particle discrimination procedure to detect margin fallers and splashing and to discriminate between rain, graupel, and hail. Margin fallers are identified when particles are observed to have a fall velocity 60% above the values typically observed for rain and hail (hatched area in Fig. B1, denoted as margin fallers). Splashing is identified when fall velocities are below 60% of the rain line and  $d < 2$  mm (hatched area in Fig. B1, denoted as splashing). Particles can be identified as rain, graupel, and hail (gray areas in Fig. B1) when the particles are sorted with  $\pm 60\%$  of the typical fall velocity–diameter relationship [solid gray lines in Fig. B1; relationships are listed in Friedrich et al. (2013)]. To avoid misclassifying spurious raindrops as graupel, the upper level of the

graupel class is reduced to the fall velocity–diameter relationship for graupel. Particles between 5 and 8 mm can be classified either as rain or hail depending on their fall velocities.

## REFERENCES

- Atlas, D., R. C. Srivastava, and R. S. Sekhon, 1973: Doppler radar characteristics of precipitation at vertical incidence. *Rev. Geophys.*, **11**, 1–35.
- Battaglia, A., E. Rustemeier, A. Tokay, U. Blahak, and C. Simmer, 2010: PARSIVEL snow observations: A critical assessment. *J. Atmos. Oceanic Technol.*, **27**, 1400–1416.
- Berg, R., 2009: Tropical cyclone report, Hurricane Ike. National Hurricane Center Tech. Rep. AL092008, 55 pp.
- Berne, A., and R. Uijlenhoet, 2005: Quantification of the radar reflectivity sampling error in non-stationary rain using paired disdrometers. *Geophys. Res. Lett.*, **32**, L19813, doi:10.1029/2005GL024030.
- Bradley, S. G., and C. D. Stow, 1975: Reply. *J. Appl. Meteor.*, **14**, 426–428.
- Brawn, D., and G. Upton, 2008: On the measurement of atmospheric gamma drop-size distributions. *Atmos. Sci. Lett.*, **9**, 245–247.
- Bringi, V. N., V. Chandrasekar, J. Hubbert, E. Gorgucci, W. L. Randeu, and M. Schoenhuber, 2003: Raindrop size distribution in different climatic regimes from disdrometer and dual-polarized radar analysis. *J. Atmos. Sci.*, **60**, 354–365.
- Brown, M. J., and E. L. Peck, 1962: Reliability of precipitation measurements as related to exposure. *J. Appl. Meteor.*, **1**, 203–207.
- Caracciolo, C., F. Rodi, and R. Uijlenhoet, 2006: Comparison between Pluix and impact/optical disdrometers during rainfall measurement campaigns. *Atmos. Res.*, **82**, 137–163.
- Coutinho, M. A., and P. P. Tomás, 1995: Characterization of raindrop size distributions at the Vale Formoso Experimental Erosion Center. *Catena*, **25**, 187–197.
- Crewell, S., and Coauthors, 2008: The general observation period 2007 within the priority program on quantitative precipitation forecasting: Concept and first results. *Meteor. Z.*, **17**, 849–866.
- Friedrich, K., E. A. Kalina, F. J. Masters, and C. R. Lopez, 2013: Drop-size distributions in thunderstorms measured by optical disdrometers during VORTEX2. *Mon. Wea. Rev.*, **141**, 1182–1203.
- Goddard, J. W. F., and S. M. Cherry, 1984: The ability of dual-polarization radar (copolar linear) to predict rainfall rate and microwave attenuation. *Radio Sci.*, **19**, 201–208.
- , —, and V. N. Bringi, 1982: Comparison of dual-polarization radar measurements of rain with ground-based disdrometer measurements. *J. Appl. Meteor.*, **21**, 252–256.
- Griffiths, R. F., 1975: Comments on “The measurement of charge and size of raindrops: Parts I and II.” *J. Appl. Meteor.*, **14**, 422–425.
- Gunn, R., and G. D. Kinzer, 1949: The terminal velocity of fall for water droplets in stagnant air. *J. Meteor.*, **6**, 243–248.
- Hall, R. L., and I. R. Calder, 1993: Drop size modification by forest canopies: Measurements using a disdrometer. *J. Geophys. Res.*, **98** (D10), 18 465–18 470.
- Jaffrain, J., and A. Berne, 2011: Experimental quantification of the sampling uncertainty associated with measurements from PARSIVEL disdrometers. *J. Hydrometeorol.*, **12**, 352–370.

- Jorgensen, D. P., and P. T. Willis, 1982: A Z-R relationship for hurricanes. *J. Appl. Meteor.*, **21**, 356–366.
- Krajewski, W. F., and Coauthors, 2006: DEVEX—Disdrometer evaluation experiment: Basic results and implications for hydrologic studies. *Adv. Water Resour.*, **29**, 311–325.
- Kruger, A., and W. F. Krajewski, 2002: Two-dimensional video disdrometer: A description. *J. Atmos. Oceanic Technol.*, **19**, 602–617.
- Löffler-Mang, M., and J. Joss, 2000: An optical disdrometer for measuring size and velocity of hydrometeors. *J. Atmos. Oceanic Technol.*, **17**, 130–139.
- , and U. Blahak, 2001: Estimation of the equivalent radar reflectivity factor from measured snow size spectra. *J. Appl. Meteor.*, **40**, 843–849.
- Lopez, C. R., F. J. Masters, and K. Friedrich, 2011: Capture and characterization of wind-driven rain during tropical cyclones and supercell thunderstorms. *Proc. 13th Int. Conf. on Wind Engineering*, Amsterdam, Netherlands, EWEA, 4 pp.
- Lyth, D., 2008: Results from UK Met Office investigations into new technology present weather sensors. *Proc. WMO Technical Conf. on Instruments and Methods of Observation*, IOM 96 (TD 1462), St. Petersburg, Russia, WMO, 13 pp. [Available online at [http://www.wmo.int/pages/prog/www/IMOP/publications/IOM-96\\_TECO-2008/2%2816%29\\_Lyth\\_United\\_Kingdom.doc](http://www.wmo.int/pages/prog/www/IMOP/publications/IOM-96_TECO-2008/2%2816%29_Lyth_United_Kingdom.doc).]
- Maeso, J., V. N. Bringi, S. Cruz-Pol, and V. Chandrasekar, 2005: DSD characterization and computations of expected reflectivity using data from a two-dimensional video disdrometer deployed in a tropical environment. *Proc. Int. Geoscience and Remote Sensing Symp.*, Seoul, South Korea, IEEE, 5073–5076.
- Matrosov, S. Y., C. Campbell, D. Kingsmill, and E. Sukovich, 2009: Assessing snowfall rates from X-band radar reflectivity measurements. *J. Atmos. Oceanic Technol.*, **26**, 2324–2339.
- McFarquhar, G. M., and R. A. Black, 2004: Observations of particle size and phase in tropical cyclones: Implications for mesoscale modeling of microphysical processes. *J. Atmos. Sci.*, **61**, 422–439.
- Merceret, F. J., 1974a: On the size distribution of raindrops in Hurricane Ginger. *Mon. Wea. Rev.*, **102**, 714–716.
- , 1974b: A note on the vertical distribution of raindrop size spectra in Tropical Storm Felice. *Meteor. Mag.*, **103**, 358–360.
- Moisseev, D., T. L'Ecuyer, W. Petersen, M. Schwaller, D. Hudak, J. Poutiainen, J. Koskinen, and V. Chandrasekar, 2009: Light precipitation validation experiment: Goals and instrumentation. *Extended Abstracts, Eighth Int. Symp. on Tropospheric Profiling*, Delft, Netherlands, CETEMPS, S12-P06. [Available online at <ftp://ftp.sma.ch/outgoing/dcr/ISTP/ABSTRACTS/data/1712609.pdf>.]
- Nešpor, V., W. F. Krajewski, and A. Kruger, 2000: Wind-induced error of raindrop size distribution measurement using a two-dimensional video disdrometer. *J. Atmos. Oceanic Technol.*, **17**, 1483–1492.
- Niu, S., X. Jia, J. Sang, X. Liu, C. Lu, and Y. Liu, 2010: Distributions of raindrop sizes and fall velocities in a semiarid plateau climate: Convective versus stratiform rains. *J. Appl. Meteor. Climatol.*, **49**, 632–645.
- Raasch, J., and H. Umhauer, 1984: Errors in the determination of particle size distributions caused by coincidences in optical particle counters. *Part. Part. Syst. Character.*, **1**, 53–58.
- Saffir, H., 1975: *Low Cost Construction Resistant to Earthquakes and Hurricanes*. United Nations, 205 pp.
- Schuur, T. J., A. V. Ryzhkov, D. S. Zrnic, and M. Schoenhuber, 2001: Drop size distributions measured by a 2D video disdrometer: Comparison with dual-polarization radar data. *J. Appl. Meteor.*, **40**, 1019–1034.
- Simpson, R. H., 1974: The hurricane disaster—Potential scale. *Weatherwise*, **27**, 169–186.
- Sugiura, K., T. Ohata, and D. Yang, 2006: Catch characteristics of precipitation gauges in high-latitude regions with high winds. *J. Hydrometeorol.*, **7**, 984–994.
- Testud, J., S. Oury, R. A. Black, P. Amayenc, and X. Dou, 2001: The concept of “normalized” distribution to describe raindrop spectra: A tool for cloud physics and cloud remote sensing. *J. Appl. Meteor.*, **40**, 1118–1140.
- Thurai, M., and V. N. Bringi, 2005: Drop axis ratios from a 2D video disdrometer. *J. Atmos. Oceanic Technol.*, **22**, 966–978.
- , W. A. Petersen, and L. D. Carey, 2010: DSD characteristics of cool-season tornadic storm using C-band polarimetric radar and two 2D-video disdrometers. *Extended Abstracts, Sixth European Conf. on Radar in Meteorology and Hydrology*, Sibiu, Romania, EMS. [Available online at [http://www.erad2010.org/pdf/oral/tuesday/radpol1/5\\_ERAD2010\\_0101.pdf](http://www.erad2010.org/pdf/oral/tuesday/radpol1/5_ERAD2010_0101.pdf).]
- , —, A. Tokay, C. Schultz, and P. Gatlin, 2011: Drop size distribution comparisons between PARSIVEL and 2-D video disdrometers. *Adv. Geosci.*, **30**, 3–9.
- Tokay, A., D. A. Short, C. R. Williams, W. L. Ecklund, and K. S. Gage, 1999: Tropical rainfall associated with convective and stratiform clouds: Intercomparison of disdrometer and profiler measurements. *J. Appl. Meteor.*, **38**, 302–320.
- , A. Kruger, and W. F. Krajewski, 2001: Comparison of drop size distribution measurements by impact and optical disdrometers. *J. Appl. Meteor.*, **40**, 2083–2097.
- , P. G. Bashor, and K. R. Wolff, 2005: Error characteristics of rainfall measurements by collocated Joss–Waldvogel disdrometers. *J. Atmos. Oceanic Technol.*, **22**, 513–527.
- , —, E. Habib, and T. Kasparis, 2008: Raindrop size distribution measurements in tropical cyclones. *Mon. Wea. Rev.*, **136**, 1669–1685.
- Ulbrich, C. W., 1983: Natural variations in the analytical form of the raindrop size distribution. *J. Climate Appl. Meteor.*, **22**, 1764–1775.
- , and L. G. Lee, 2002: Rainfall characteristics associated with the remnants of Tropical Storm Helene in upstate South Carolina. *Wea. Forecasting*, **17**, 1257–1267.
- Wang, P. K., and H. R. Pruppacher, 1977: Acceleration to terminal velocity of cloud and raindrops. *J. Appl. Meteor.*, **16**, 275–280.
- Weiss, L. L., 1961: Relative catches of snow in shielded and unshielded gages at different wind speeds. *Mon. Wea. Rev.*, **89**, 397–400.
- Wilson, J. W., and D. M. Pollock, 1974: Rainfall measurements during Hurricane Agnes by three overlapping radars. *J. Appl. Meteor.*, **13**, 835–844.
- Wurman, J., D. Dowell, Y. Richardson, P. Markowski, E. Rasmussen, D. Burgess, L. Wicker, and H. Bluestein, 2012: The second Verification of the Origins of Rotation in Tornadoes Experiment: VORTEX2. *Bull. Amer. Meteor. Soc.*, **93**, 1147–1170.
- Yang, D., B. E. Goodison, J. R. Metcalfe, V. S. Golubev, R. Bates, T. Pangburn, and C. L. Hanson, 1998: Accuracy of NWS 8” standard nonrecording precipitation gauge: Results and application of WMO intercomparison. *J. Atmos. Oceanic Technol.*, **15**, 54–68.
- Yuter, S. E., D. E. Kingsmill, L. B. Nance, and M. Löffler-Mang, 2006: Observations of precipitation size and fall speed characteristics within coexisting rain and wet snow. *J. Appl. Meteor. Climatol.*, **45**, 1450–1464.